# The Huggins band of ozone: Unambiguous electronic and vibrational assignment

Zheng-Wang Qu, Hui Zhu, Motomichi Tashiro, and Reinhard Schinke[a)]
*Max-Planck-Institut für Strömungsforschung, D-37073 Göttingen, Germany*

Stavros C. Farantos
*Institute of Electronic Structure and Laser Foundation for Research and Technology-Hellas, and Department of Chemistry, University of Crete, Iraklion 711 10, Crete, Greece*

(Received 12 February 2004; accepted 2 March 2004)

The Huggins band of ozone is investigated by means of exact dynamics calculations using a new (diabatic) potential energy surface for the $^1B_2$ state. The remarkable agreement with the measured spectrum strongly suggests that the Huggins band is due to the two $C_s$ potential wells of the $^1B_2$ state. The vibrational assignment, based on the nodal structure of wave functions, supports the most recent experimental assignment. © *2004 American Institute of Physics.*
[DOI: 10.1063/1.1711589]

Because of the importance of ozone for the shielding of harmful UV light, its photophysics has been intensively studied.[1–3] Nevertheless, there are still several aspects which are not completely understood. One open question concerns the electronic and vibrational assignment of the Huggins band ($310\ \text{nm} \lesssim \lambda \lesssim 370\ \text{nm}$), which was first observed more than a century ago.[4] This absorption band is located at the very red tail of the strong Hartley band. The cross section is exceedingly small but increases by about four orders of magnitude within the range of the Huggins band. It shows a long progression of diffuse vibrational structures, the assignment of which has been debated for a long time; the ''history'' of this assignment recently was reviewed by O'Keeffe *et al.*[5] Several points make a clear-cut assignment of the Huggins band difficult: doubts about the upper electronic state and therefore the topography of the relevant potential energy surface (PES), the diffuseness of the absorption features, and congestion because of hot bands.

Concerning the upper electronic state there are two principle possibilities: the second or the third singlet $^1A'$ state, $2\,^1A'$ ($2\,^1A_1$) or $3\,^1A'$ ($1\,^1B_2$), where the notations in parentheses quote the electronic symmetry in $C_{2v}$ geometry; the ordering of states refers to the equilibrium geometry of the ground state $\tilde{X}\,^1A'$ ($^1A_1$). Figure 1(b) illustrates the ordering of states by showing cuts through the PESs of the lowest five $^1A'$ electronic states. The second state, called *A* according to Hay *et al.*,[6] has one minimum, located at the $C_{2v}$ symmetry line ($R_1 = R_2$), whereas the third state (*B*) has two $C_s$ minima with one bond length being substantially longer than the other one.[6–9] In what follows, $R_1$ and $R_2$ denote the bond distances between the central oxygen atom and the two outer ones and $\alpha$ is the OOO bond angle. States *A* and *B* have an avoided crossing in the energy range of the Huggins band. Both states asymptotically correlate with excited products, namely, $O(^1D)$ and $O_2(a\,^1\Delta_g)$. They are crossed by a higher electronic state, referred to as *R*, which correlates with ground state products $O(^3P)$ and $O_2(X\,^3\Sigma_g^-)$.

The very strong Hartley band is due to the $B \leftarrow X$ transition. In Ref. 9, arguments were given which speak against the *A* state as the origin of the Huggins band. The main one is the angle dependence of the corresponding PES: The *A* state correlates with cyclic ozone with $D_{3h}$ symmetry, which has its equilibrium at $\alpha = 60°$. Thus, if the *A* state were excited, a very long bending progression would be expected,

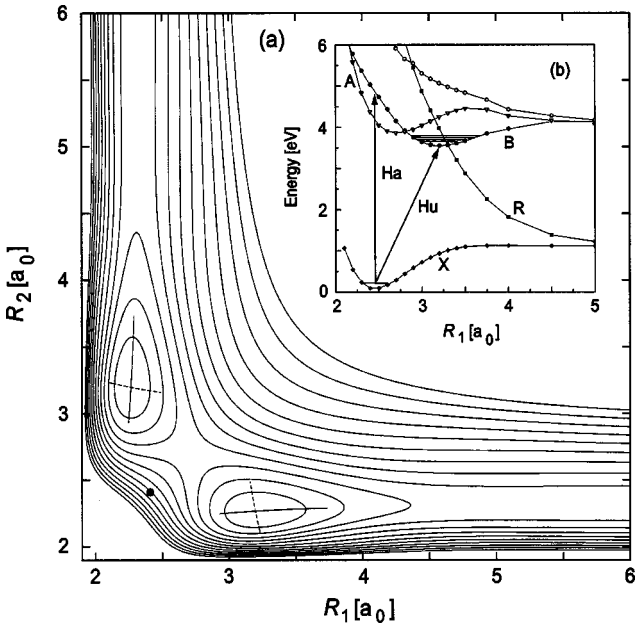


FIG. 1. (a) Two-dimensional representation of the *B*-state PES as function of the two OO bond distances; the bond angle is 110°. The filled circle marks the FC point and the lines indicate the classical periodic orbits for the long-bond stretch ($S_1$, solid line) and the short-bond stretch ($S_3$, dashed line), respectively. (b) One-dimensional potential cuts of the five lowest $^1A'$ states (original *ab initio* data). *A*, *B*, *R*, and *X* denote the relevant diabatic states as described in the text. Energy normalization is with respect to the minimum of the ground state.

[a)]Electronic address: rschink@gwdg.de

 

TABLE I. Stationary points of the fitted *B*-state potential energy surface.

| | $R_1$[a] | $R_2$ | $\alpha$ | $E$ |
|---|---|---|---|---|
| Minimum | 3.221 | 2.258 | 109.5 | 3.429 |
| Saddle | 2.704 | 2.704 | 109.5 | 4.108 |
| $O(^1D)+O_2(a\ ^1\Delta_g)$ | $\infty$ | 2.316 | $\cdots$ | 4.046 |

[a]Distances in $a_0$ and angles in degrees; energy is normalized with respect to the minimum of the ground state.

because the equilibrium angle of the *X* state is 117°. The observed bending progression, however, is rather short.[5]

In the present study we perform dynamics calculations using a new PES for the *B* state and demonstrate that the resulting spectrum of vibrational energies in the two $C_s$ wells as well as the corresponding intensities are in good agreement with the experimental spectrum. Our vibrational assignment mostly agrees with that of O'Keeffe *et al.*,[5] which is the latest and the most complete experimental assignment. We disagree, however, in the electronic assignment. O'Keeffe *et al.*[5] attributed the Huggins band to the *A* state, mainly because the only *B*-state PES available at that time—the PES of Yamashita *et al.*[7,10] (YMLL)—appeared to be in quantitative disagreement with their analysis. The YMLL PES has been used in two dynamics studies in order to explain the Huggins band.[11,12] Although some qualitative aspects of the spectrum have been reproduced, these calculations leave a number of questions unanswered (e.g., vibrational assignments, intensities, hot bands, and the actual types of vibrational motions associated with the stretching modes).

The electronic structure calculations are identical to those described by Qu *et al.*:[9] internally contracted multireference configuration interaction calculations together with Dunning's standard augmented correlation consistent triple-zeta basis set.[13] The CI wave functions are based on state-averaged complete active space self-consistent field (CASSCF) orbitals with 18 electrons in 12 orbitals (full-valence active space) and three fully optimized closed-shell inner orbitals. The five lowest $^1A'$ states are included, which makes the calculations very demanding. All three coordinates are varied and the transition dipole moment function (TDM) with the ground state is also determined. All calculations are carried out with the MOLPRO suite of programs.[14]

A complete description of the photodissociation of ozone in the UV requires taking into account at least three $^1A'$ states—*A*, *B*, and *R*—as well as several triplet states, which cross the singlet states at energies in the energy range of the Huggins band.[15] Such a multistate calculation is beyond our possibilities. Instead, we construct a *diabatic* PES for the *B* state, where the diabatization is done by simply connecting appropriate points on both sides of the avoided crossing.[6,9] This is justified for our present purpose, because the mixing between *B* and *A* as well as *B* and *R* is weak in the region of the well of the *B* state. The potential energies selected in this way are fitted to an analytical expression, which is symmetric in all three bond lengths. In the fitting points with energies in the range of the well are given the highest weights. Figure 1(a) depicts a 2D cut and the characteristic data of the fitted PES are collected in Table I.

TABLE II. Calculated vibrational energies $E$ (in eV), transition frequencies $E_{(v_1,v_2,v_3)}$ (in $cm^{-1}$), deviations from measured transition frequencies (Table I of Ref. 5), and calculated relative intensities $I$.

| No. | $(v_1,v_2,v_3)$ | $E$[a] | $E_{(v_1,v_2,v_3)}$ | Expt.-Calc. | $I$ |
|---|---|---|---|---|---|
| 1 | 000 | 3.5952 | 0 | 0 | 1.0 |
| 3 | 100 | 3.6823 | 702.4 | 4 | 9.3 |
| 5 | 110 | 3.7281 | 1071.6 | −15 | 11.6 |
| 7 | 200 | 3.7655 | 1373.9 | −21 | 42.6 |
| 8 | 120[b] | 3.7730 | 1434.2 | −26 | 13.8 |
| 11 | 210 | 3.8090 | 1724.7 | −34 | 64.5 |
| 12 | 130[b] | 3.8171 | 1789.7 | −32 | 15.4 |
| 15 | 300 | 3.8447 | 2012.5 | −42 | 120.9 |
| 16 | 220 | 3.8517 | 2068.4 | −34 | 90.3 |
| 17 | 140[b] | 3.8602 | 2137.7 | −51 | 18.4 |
| 21 | 310 | 3.8857 | 2343.4 | −43 | 211.6 |
| 22 | 230[b] | 3.8934 | 2404.7 | −43 | 115.2 |
| 26 | 400 | 3.9195 | 2615.5 | −67 | 226.6 |
| 28 | 320 | 3.9259 | 2666.9 | −55 | 339.4 |
| 29 | 240[b] | 3.9340 | 2733.0 | −63 | 147.9 |
| 35 | 410 | 3.9579 | 2925.5 | −63 | 446.9 |
| 36 | 330 | 3.9649 | 2981.7 | −58 | 382.5 |
| 38 | 250[b] | 3.9737 | 3052.4 | −68 | 183.6 |
| 40 | 500 | 3.9886 | 3173.2 | −76 | 53.6 |

[a]Normalization of energy is made with respect to the minimum of the ground state.
[b]Experimental energy obtained from a hot band.

Two types of dynamics calculations—all for $J=0$—have been performed: filter diagonalization[16,17] and harmonic inversion.[18] The filter diagonalization method is used to calculate the energies and wave functions (for assignments), whereas the harmonic inversion approach is used to calculate energies and intensities. The coordinates are the same Jacobi coordinates as employed for calculating the energies for the ground state.[19] They take into account the $C_{2v}$ symmetry of the PES. The wave functions are either symmetric or antisymmetric with respect to the $C_{2v}$ line. Because the energies considered in this study are well below the saddle between the two $C_s$ wells, the splittings between the symmetric and the antisymmetric eigenenergies are marginally small. Franck–Condon (FC) factors, including the TDM function, are calculated for the states $(0,0,0)_X$, $(1,0,0)_X$, $(0,1,0)_X$ and $(0,0,1)_X$ in the ground electronic state. Because of the restriction to $J=0$ and the neglect of coupling to other electronic states leading to substantial broadening, absolute absorption cross sections have not been calculated.

In Table II we compare the calculated vibrational excitation energies with the experimental ones of Katayama,[20] on which the assignment of O'Keeffe *et al.*[5] is based. Only those calculated energies are listed here for which there is an experimental counterpart. The theoretical assignment is based on visual inspection of the wave functions and counting the nodes. For the states included in Table II it is unambiguous. For higher energies, however, the assignment becomes less and less clear because of state mixings. There is a one-to-one correspondence between the experimental and the theoretical assignments in Table II, which confirms the assignment of O'Keeffe *et al.*[5] The older experimental assignments differ significantly, mainly in the number of bending and ''antisymmetric'' stretch excitations.[5,20–24] In view of the limited accuracy of the electronic structure calculations, the

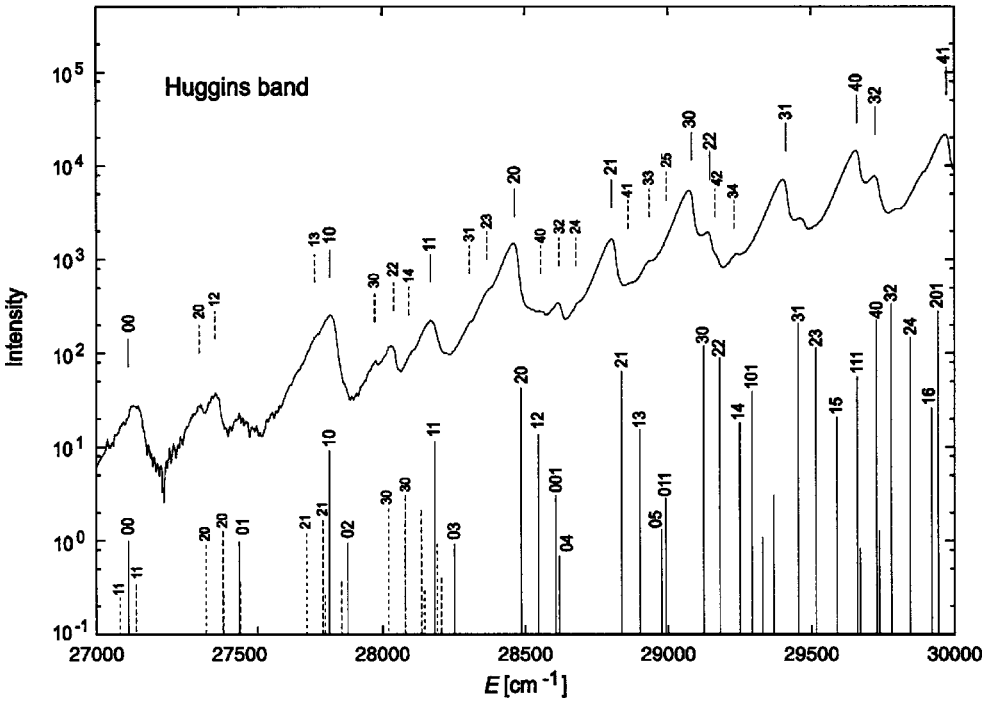


FIG. 2. The absorption cross section of ozone in the region of the Huggins band (arbitrary units). The continuous curve represents the measured cross section of Malicet *et al.* for 218 K (Ref. 25). The numbers above the experimental spectrum give the assignments due to O'Keeffe *et al.* (Ref. 5) where the dashed vertical lines indicate hot bands. The stick spectrum shows the calculated FC factors [normalized such that $I=1$ for (0,0,0)]. If only two quantum numbers are quoted, $v_3$ is equal to zero. Also a few calculated hot bands (for 250 K) are presented in the lower part of the spectrum. Short/long dashes indicate transitions originating from the $(1,0,0)_X/(0,0,1)_X$ state in the ground electronic state. The theoretical spectrum is shifted so that the (0,0,0) band agrees with the experimental origin.

restriction to $J=0$ and one state, as well as the diffuseness of the measured spectrum the agreement is very good. It is similar for $^{18}O_3$. The calculated energy for the transition $(0,0,0)_B \leftarrow (0,0,0)_X$ for $^{16}O_3$ is 27 520 $cm^{-1}$ compared to the measured energy of 27 112 $cm^{-1}$.[5,20]

Our interpretation of the stretching vibrational modes differs from the previous interpretations. While O'Keeffe *et al.*,[5] like most others who dealt with the assignment of the Huggins band, attributed to the modes $\nu_1$ and $\nu_3$ symmetric and antisymmetric stretch motion—which is correct for the *X* state—, we interprete them as *long-bond* and *short-bond* excitation (local modes) as illustrated by classical periodic orbits in Fig. 1. The quantum numbers $v_1$ and $v_3$ count the number of nodes along $S_1$ and $S_3$, respectively. They refer to excitation in only *one* of the two (identical) potential wells. Because the first mode describes motion along the dissociation path, it is quite anharmonic. The short-bond stretch is similar to the vibration of the free oxygen molecule and the frequency is similar to that of $O_2(a^1\Delta_g)$. The second mode is—in our assignment as well as in all previous assignments—the bending mode.

The absorption cross section is exceedingly small because only the exponential tails of the ground- and the excited-state wave functions overlap. However, excitation of the $\nu_1$ mode strongly enhances the overlap and therefore the intensity rapidly increases with $\nu_1$ as seen in Table II. On the other hand, pure excitation of the short-bond stretch and the bending mode do not significantly increase the FC overlap. The situation becomes more involved, however, at higher energies when the mixing of states is stronger.

The overall intensity pattern of the calculated (stick) spectrum agrees well with the measured spectrum[25] as demonstrated in Fig. 2. Especially, the nearly exponential increase with energy is satisfactorily reproduced. This is important because it underlines that excitation from the ground state to the $C_s$ wells of the *B* state is possible, even though the equilibrium geometries are very different. Although we agree with most of the assignments of O'Keeffe *et al.*,[5] there are some differences, mainly concerning hot bands. The two peaks around 27 400 $cm^{-1}$ have been assigned to the states (2,0,0) and (1,2,0) both excited from the $(1,0,0)_X$ state. We assign them to (2,0,0) starting, however, from states $(1,0,0)_X$ and $(0,0,1)_X$. Both, symmetric stretch and antisymmetric stretch in the *X* state strongly increase the overlap with the *B*-state wave functions; the increase is more pronounced for excitation of the antisymmetric stretch motion. Thus, the gap between the two peaks corresponds to the separation between $(1,0,0)_X$ and $(0,0,1)_X$ of about 60 $cm^{-1}$. Other pairs of similar hot bands are clearly seen in the low-energy regime of the spectrum, for example, around 28 100 $cm^{-1}$. The theoretical spectrum in Fig. 2 shows several hot bands calculated using the appropriate Boltzmann factors. In order to avoid overcrowding of the figure, hot bands only up to about 28 300 $cm^{-1}$ are shown; nevertheless, hot bands make significant contributions to the spectrum also at higher energies, e.g., at both sides of the (2,0,0) peak.

In addition to rotational broadening, the widths of the spectral features in the experimental spectrum reflect predissociation by nonadiabatic coupling to the repulsive *R* state or by spin–orbit coupling to the triplet states, which cross the *B*

state.[15] Therefore, in order to correctly describe the linewidths a multistate calculation is necessary. This is not attempted here.

The good agreement obtained—without any adjustable parameter—for (1) the origin of the Huggins band, (2) the vibrational energies for $^{16}O_3$ and for $^{18}O_3$, (3) the assignments of hot bands, and (4) the intensity patterns strongly suggests that our calculations with only the (diabatic) PES for the *B* state provides a realistic description of the dynamics in the Huggins band and ascertains that the Huggins band is due to a transition to the $C_s$ wells of the *B* state, i.e., the same state responsible for the Hartley band. A longstanding puzzle of the UV spectrum of ozone is resolved. In a forthcoming publication we will present details of the calculations, the assignment of the spectrum up to higher energies and its temperature dependence, and the results for $^{18}O_3$. In addition, a detailed analysis of the classical phase space will be presented.

Financial support by the Deutsche Forschungsgemeinschaft is gratefully acknowledged. The authors are indebted to S. Yu. Grebenshchikov for invaluable help in the dynamics calculations. They are grateful to Dr. Malicet for providing the experimental absorption cross section shown in Fig. 2.

[1] P. L. Houston, "Photodissociation dynamics of ozone in the Hartley band," in *Advanced Series in Physical Chemistry Modern Trends in Chemical Reaction Dynamics*, edited by K. Liu and X. Yang (World Scientific, Singapore, 2003).
[2] J. Orphal, J. Photochem. Photobiol. **157**, 185 (2003).
[3] Y. Matsumi and M. Kawasaki, Chem. Rev. **103**, 4767 (2003).
[4] W. Huggins and Mrs. Huggins, Proc. R. Soc. London **48**, 216 (1890).
[5] P. O'Keeffe, T. Ridley, K. P. Lawley, and R. J. Donovan, J. Chem. Phys. **115**, 9311 (2001).
[6] P. J. Hay, R. T. Pack, R. B. Walker, and E. J. Heller, J. Phys. Chem. **86**, 862 (1982).
[7] K. Yamashita, K. Morokuma, F. LeQuéré, and C. Leforestier, Chem. Phys. Lett. **191**, 515 (1992).
[8] A. Banichevich, S. D. Peyerimhoff, and F. Grein, Chem. Phys. **178**, 155 (1993).
[9] Z.-W. Qu, H. Zhu, and R. Schinke, Chem. Phys. Lett. **377**, 359 (2003).
[10] C. Leforestier, F. LeQuéré, K. Yamashita, and K. Morokuma, J. Chem. Phys. **101**, 3806 (1994).
[11] F. LeQuéré and C. Leforestier, Chem. Phys. Lett. **189**, 537 (1992).
[12] O. Bludský and P. Jensen, Mol. Phys. **91**, 653 (1997).
[13] T. H. Dunning, Jr., J. Chem. Phys. **90**, 1007 (1989).
[14] MOLPRO is a package of *ab initio* programs written by H.-J. Werner and P. J. Knowles. Further information can be obtained from http://www.tc.bham.ac.uk/molpro/
[15] H. Zhu, Z.-W. Qu, M. Tashiro, and R. Schinke, Chem. Phys. Lett. **384**, 45 (2004).
[16] T. P. Grozdanov, V. A. Mandelshtam, and H. S. Taylor, J. Chem. Phys. **103**, 7990 (1995).
[17] M. R. Wall and D. Neuhauser, J. Chem. Phys. **102**, 8011 (1995).
[18] V. A. Mandelshtam and H. S. Taylor, J. Chem. Phys. **106**, 5085 (1997).
[19] R. Siebert, P. Fleurat-Lessard, R. Schinke, M. Bittererová, and S. C. Farantos, J. Chem. Phys. **116**, 9749 (2002).
[20] D. H. Katayama, J. Chem. Phys. **71**, 815 (1979).
[21] A. Jakowlewa and V. Kondratjew, Phys. Z. Sowjetunion **9**, 106 (1936).
[22] J. W. Simons, R. J. Paur, H. A. Webster III, and E. J. Bair, J. Chem. Phys. **59**, 1203 (1973).
[23] J. C. D. Brand, K. J. Cross, and A. R. Hoy, Can. J. Phys. **56**, 327 (1978).
[24] J. A. Joens, J. Chem. Phys. **101**, 5431 (1994).
[25] J. Malicet, D. Daumont, J. Charbonnier, C. Parisse, A. Chakir, and J. Brion, J. Atmos. Chem. **21**, 263 (1995).